JOURNAL OF COMPUTATIONAL PHYSICS **123,** 119–126 (1996)
ARTICLE NO. 0010

Improved Solutions to the Small Strain Continuum Equations Using a Modified Engquist Filter

C. K. B. LEE AND R. C. CRAWFORD

Logicon RDA, Los Angeles, California 90009

AND

J. M. MCDONOUGH

University of Kentucky, Lexington, Kentucky 40506-0108

Received October 7, 1994; revised June 7, 1995

For wave propagation problems in linear and bilinear elastic solids and a class of simple nonlinear solids the benefits of high-resolution schemes in gasdynamics can be immediately extended to solid mechanics. The Engquist filter for the system of conservation laws in gasdynamics is extended to solid mechanics and implemented in a finite-difference code. The present results show that highly resolved numerical solutions, i.e., sharp shocks with very little oscillation behind them, can be achieved by applying this nonlinear filter to the finite-difference solution at every timestep. Plane wave propagation in three types of solids is calculated by the LAYER code. A two-dimensional grid is used to compute these one-dimensional plane wave problems. For linear elastic solids the nonlinear filter performed very well in removing the Gibbs oscillations. For bilinear solids the numerical solution is compared to a known analytical solution. Because this analytical solution involves a planar shock with a decaying pressure behind it, the existing form of the Engquist filter (designed for a constant pressure behind the shock) has to be modified. The relationship between this modified filter and the flux modification in the TVD scheme is discussed. This modification is expected to be necessary when the filter is applied to multi-dimensional problems. The potential for obtaining highly resolved shocks from classical second-order finite-difference solid mechanics codes using the modified nonlinear filter is demonstrated.

1. INTRODUCTION

In the last decade, a set of high-resolution numerical schemes for gasdynamics [1–4] has emerged. The most notable feature in these schemes is their ability to produce sharp shocks without spurious oscillations. Although these methods are derived from very different concepts, all of them manage to introduce, in one form or another, a judicious amount of dissipation at chosen locations in the flow field to reduce numerical oscillations. For example, limiters are used in the TVD scheme of Harten [1] and the FCT method of Zalesak [2], and switches and cell-averaged piecewise fits are used in the PPM (Colella and Woodward [3]) and ENO (Harten and Osher [4]) schemes. Later in the decade, Engquist *et al.* [5] proposed yet another method of introducing the required amount of dissipation, namely, the use of nonlinear filters. The advantage of these filters is that they can be implemented into existing finite-difference codes. These filters can be constructed to satisfy any set of criteria required by the high-resolution schemes. For example, the filter can be constructed to satisfy the monotonicity preserving requirement of the TVD scheme, or it can be constructed to satisfy the criteria leading to ENO schemes [6]. Using these filters, the properties of the high-resolution schemes can be implemented into a finite-difference code allowing the analyst to choose the best numerical approach for a given problem. This is a better investment than having to develop a new set of codes that uses the individual schemes. Moreover, the computing cost of these newer schemes is at least a factor of several higher than finite difference schemes. The main reason for the higher cost is the characteristic decomposition [7], the Riemann solver or approximate Riemann solver [8], and the high-order fits to the solution. For some problems, the advanced schemes can be an order of magnitude more costly. The advantage of the filter, in this case, is that typically only a relatively small number of grid points need be modified by the filter, resulting in substantial savings in computer time.

The first attempt in extending an advanced gasdynamics scheme to continuum mechanics is by Antman and Szymczak [9] who applied the higher-order Godunov technique to the longitudinal motion of an elastoplastic bar in one dimension. This is followed by the work of Trangenstein and Colella [10] who extended the higher-order Godunov technique to elastic-plastic solids in general. Detailed characteristics analyses, for both the Eulerian and the Lagrangian frames of reference, are included in their evaluation of the compatibility of their higher-order Godunov scheme and continuum mechanics. Because they [10] have taken such a general approach, even though

0021-9991/96 $12.00

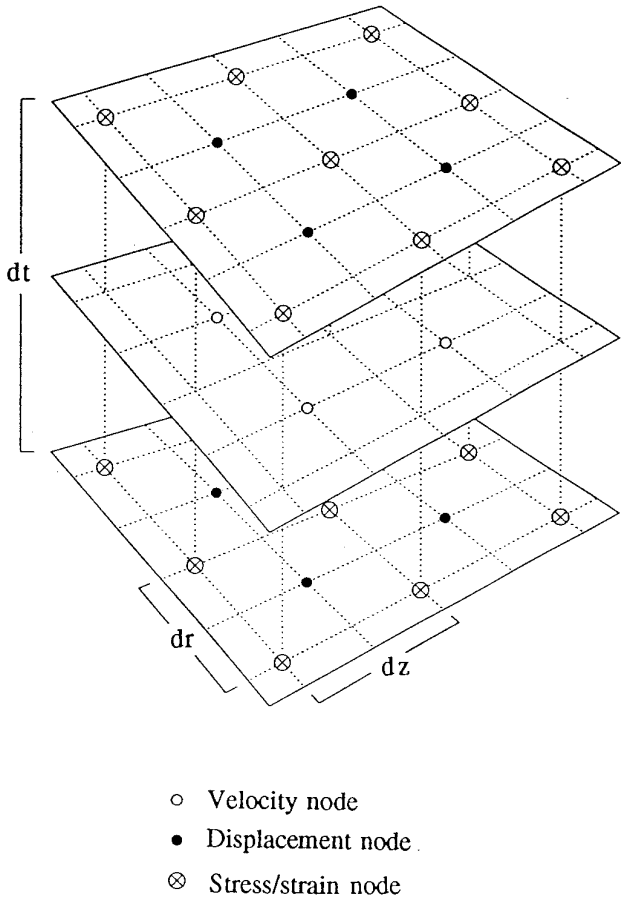

FIG. 1. Time step and spacial grid layout for the LAYER code. Nodes indicate the variables being calculated.

significant progress has been made, it will still be some time before the practical engineers can benefit from this technology. Moreover, from [9, 10] it appears that extending a high-resolution scheme for gasdynamics to solid mechanics is quite involved. This raises serious questions as to whether these high-resolution shock capturing schemes can enjoy the same success in solids as in gasdynamics. We believe that a simpler way to introduce the numerical methods giving sharp shocks with very little oscillations in existing industrial codes is through the Engquist filter. We will show in this paper that even this simpler approach is somewhat involved, but for the class of wave propagation problems in solids that satisfies the small strain constraint, the benefits of these advanced numerical techniques can be extended to solid mechanics immediately.

In this paper, we limit the study to linear and bilinear elastic solids and a class of simple nonlinear solids. Only plane wave propagation is considered, even though a two-dimensional grid is used in the computations. In Section 2, we show our derivation of the characteristic variables, and in Section 3, we describe this modified version of the Engquist filter. Section 4 discusses the relationship between the modified filter and the flux modification in the TVD scheme. Section 5 describes the two one-dimensional test problems. The first problem is the propagation of a square wave in a linear elastic material, while the second problem is the propagation of a planar shock in a bilinear material for which an analytical solution is available. Section 6 gives the results of the test problems as well as the solution to the case a planar shock propagating in a nonlinear solid. Section 7 presents our conclusions.

2. CHARACTERISTICS ANALYSIS

The small-strain momentum equation in two-dimensional axisymmetric Lagrangian coordinates solved in the LAYER code [11] is

$$\rho_0 \frac{\partial}{\partial t}\begin{bmatrix} v_r \\ v_z \end{bmatrix} + \frac{1}{r_0}\frac{\partial}{\partial r_0} r_0(1+\varepsilon_{\theta\theta})\begin{bmatrix} -\sigma_{rr}(1+\varepsilon_{zz}) + \sigma_{rz}(\varepsilon_{rz}-\delta_{rz}) \\ -\sigma_{rz}(1+\varepsilon_{zz}) + \sigma_{zz}(\varepsilon_{rz}-\delta_{rz}) \end{bmatrix}$$
$$+ \frac{\partial}{\partial z_0}(1+\varepsilon_{\theta\theta})\begin{bmatrix} \sigma_{rr}(\varepsilon_{rz}+\delta_{rz}) - \sigma_{rz}(1+\varepsilon_{rr}) \\ \sigma_{rz}(\varepsilon_{rz}+\delta_{rz}) - \sigma_{zz}(1+\varepsilon_{rr}) \end{bmatrix} \tag{1}$$
$$= \begin{bmatrix} (\sigma_{\theta\theta}/r_0)[(1+\varepsilon_{rr})(1+\varepsilon_{zz}) - (\varepsilon_{rz}^2 - \delta_{rz}^2)] \\ \rho_0 g \end{bmatrix},$$

and the compatibility conditions are

$$\frac{\partial \varepsilon_{rr}}{\partial t} + \frac{1}{r_0}\frac{\partial}{\partial r_0} r_0(-V_r) = -\frac{v_r}{r_0},$$
$$\frac{\partial \varepsilon_{zz}}{\partial t} + \frac{\partial}{\partial z_0}(-V_z) = 0, \tag{2}$$
$$\frac{\partial \varepsilon_{rz}}{\partial t} + \frac{1}{r_0}\frac{\partial}{\partial r_0} r_0\left(-\frac{v_z}{2}\right) + \frac{\partial}{\partial z_0}\left(-\frac{v_r}{2}\right) = -\frac{v_z}{2r_0}.$$

In writing these we used the definitions

$$\varepsilon_{rr} = \frac{\partial u_r}{\partial r_0}, \quad \varepsilon_{\theta\theta} = \frac{u_r}{r_0}, \quad \varepsilon_{zz} = \frac{\partial u_z}{\partial z_0},$$
$$\varepsilon_{rz} = \frac{1}{2}\left(\frac{\partial u_z}{\partial r_0} + \frac{\partial u_r}{\partial z_0}\right), \quad \delta_{rz} = \frac{1}{2}\left(\frac{\partial u_z}{\partial r_0} - \frac{\partial u_r}{\partial z_0}\right), \tag{3}$$

where u_r, V_r and u_z, V_z are displacements and velocities in the radial and axial directions, respectively, and r_0 and z_0 are the radial and axial Lagrangian coordinates, respectively; ρ_0 is the density at rest; g the acceleration due to gravity, and t is the time. These equations are center-differenced in both time and space (see Fig. 1) and solved in the LAYER code. Note that stresses and velocities are not given at the same location in this staggered grid.

For the two test problems the stresses are related to the strains by the linear elastic equation:

$$\begin{bmatrix}\sigma_{rr}\\ \sigma_{\theta\theta}\\ \sigma_{zz}\\ \sigma_{rz}\end{bmatrix}=\begin{bmatrix}\lambda+2\mu & \lambda & \lambda & 0\\ \lambda & \lambda+2\mu & \lambda & 0\\ \lambda & \lambda & \lambda+2\mu & 0\\ 0 & 0 & 0 & 2\mu\end{bmatrix}\begin{bmatrix}\varepsilon_{rr}\\ \varepsilon_{\theta\theta}\\ \varepsilon_{zz}\\ \varepsilon_{rz}\end{bmatrix}, \quad (4)$$

where λ and μ are Lame constants.

For the characteristics analysis in the radial direction, we collect all the terms involving the time and radial derivatives from the six equations in the left-hand side and cast all other terms to the right-hand side and combine them in a single variable $\mathbf{Q}$. For this analysis we do not need the details of $\mathbf{Q}$; we will not write it out explicitly. The resulting equation is

$$\frac{\partial}{\partial t}\begin{bmatrix}\rho_0 v_r\\ \rho_0 v_z\\ \varepsilon_{rr}\\ \varepsilon_{rz}\end{bmatrix}+\frac{\partial}{\partial r_0}\begin{bmatrix}(1+\varepsilon_{\theta\theta})[-\sigma_{rr}(1+\varepsilon_{zz})+\sigma_{rz}(\varepsilon_{rz}-\delta_{rz})]\\ (1+\varepsilon_{\theta\theta})[-\sigma_{rz}(1+\varepsilon_{zz})+\sigma_{zz}(\varepsilon_{rz}-\delta_{rz})]\\ -v_r\\ -v_z/2\end{bmatrix}=\mathbf{Q}_r. \quad (5)$$

The acoustic matrix is

$$\mathbf{A}_r=\begin{bmatrix}0 & 0 & -(\lambda+2\mu)(1+\varepsilon_{\theta\theta})(1+\varepsilon_{zz}) & 2\mu(1+\varepsilon_{\theta\theta})(2\varepsilon_{rz}-\delta_{rz})\\ 0 & 0 & \lambda(1+\varepsilon_{\theta\theta})(\varepsilon_{rz}-\delta_{rz}) & (1+\varepsilon_{\theta\theta})(\lambda\varepsilon-2\mu)\\ -1/\rho_0 & 0 & 0 & 0\\ 0 & -1/2\rho_0 & 0 & 0\end{bmatrix} \quad (6)$$

where $\varepsilon=\varepsilon_{rr}+\varepsilon_{\theta\theta}+\varepsilon_{zz}$.

The eigenvalues of $\mathbf{A}_r$ are

$$\Lambda_r^2=\frac{1+\varepsilon_{\theta\theta}}{2\rho_0}\left\{\mu-\frac{\lambda\varepsilon}{2}+(\lambda+2\mu)(1+\varepsilon_{zz})\right.$$
$$\left.\pm\sqrt{\left[\mu-(\lambda+2\mu)(1+\varepsilon_{zz})-\lambda\varepsilon/2\right]^2+4\lambda\mu(2\varepsilon_{rz}-\delta_{rz})(\varepsilon_{rz}-\delta_{rz})}\right\} \quad (7)$$

and the eigenvector associated with Λ_i is

$$\mathbf{e}_i^{\mathrm{T}}=\frac{1}{n_i}\left[1\ -\frac{2\rho_0\Lambda_i}{R_{14}}\left(\Lambda_i+\frac{R_{13}}{\rho_0\Lambda_i}\right)\right.$$
$$\left.-\frac{1}{\rho_0\Lambda_i}\ \frac{1}{R_{14}}\left(\Lambda_i+\frac{R_{13}}{\rho_0\Lambda_i}\right)\right], \quad (8)$$

where R_{13} and R_{14} are components of $\mathbf{A}_r$ and n_i is the normalization constant of the eigenvector $\mathbf{e}_i$. At this point we assemble the eigenvectors to form the eigenvector matrix $\mathbf{E}$ and calculate the inverse of $\mathbf{E}$ algebraically. This completes the preparation of the quantities needed in the characteristic decomposition.

In a similar manner we collect the time and axial derivative terms on the left-hand side and cast all other terms into $\mathbf{Q}$ in the right-hand side. We obtain

$$\frac{\partial}{\partial t}\begin{bmatrix}\rho_0 V_r\\ \rho_0 V_z\\ \varepsilon_{zz}\\ \varepsilon_{rz}\end{bmatrix}+\frac{\partial}{\partial z_0}\begin{bmatrix}(1+\varepsilon_{\theta\theta})[\sigma_{rr}(\varepsilon_{rz}+\delta_{rz})-\sigma_{rz}(1+\varepsilon_{rr})]\\ (1+\varepsilon_{\theta\theta})[\sigma_{rz}(\varepsilon_{rz}+\delta_{rz})-\sigma_{zz}(1+\varepsilon_{rr})]\\ -V_z\\ -V_r/2\end{bmatrix}=\mathbf{Q}_z. \quad (9)$$

The corresponding axial acoustic matrix is

$$\mathbf{A}_z=\begin{bmatrix}0 & 0 & \lambda(1+\varepsilon_{\theta\theta})(\varepsilon_{zz}+\delta_{rz}) & (1+\varepsilon_{\theta\theta})(\lambda\varepsilon-2\mu)\\ 0 & 0 & -(\lambda+2\mu)(1+\varepsilon_{\theta\theta})(1+\varepsilon_{rr}) & 2\mu(1+\varepsilon_{\theta\theta})(2\varepsilon_{rz}+\delta_{rz})\\ 0 & -1/\rho_0 & 0 & 0\\ -1/2\rho_0 & 0 & 0 & 0\end{bmatrix}. \quad (10)$$

The eigenvalues of this matrix are

$$\Lambda_z^2 = \frac{1+\varepsilon_{\theta\theta}}{2\rho_0}\left\{\mu - \frac{\lambda\varepsilon}{2} + (\lambda+2\mu)(1+\varepsilon_{rr}) \pm \sqrt{\left[\begin{array}{c}\mu - (\lambda+2\mu)(1+\varepsilon_{rr}) - \lambda\varepsilon/2 \\ + 4\lambda\mu(2\varepsilon_{rz}+\delta_{rz})(\varepsilon_{rz}+\delta_{rz})\end{array}\right]^2}\right\} \tag{11}$$

and the corresponding eigenvectors are

$$\mathbf{e}_i^{\mathrm{T}} = \frac{1}{n_i}\left[1 \;\; -\frac{\rho_0\Lambda_i}{z_{13}}\left(\Lambda_i + \frac{z_{14}}{2\rho_0\Lambda_i}\right) \;\; \frac{1}{z_{13}}\left(\Lambda_i + \frac{z_{14}}{2\rho_0\Lambda_i}\right) \;\; -\frac{1}{2\rho_0\Lambda_i}\right], \tag{12}$$

where z_{13} and z_{14} are components of A_z and n_i is the normalization constant. As before, we assemble the eigenvectors to form the eigenvector matrix and obtain its inverse algebraically before we call the filter subroutine.

Equations (5) and (9) can be written in the form

$$\frac{\partial \mathbf{U}}{\partial t} + \frac{\partial \mathbf{F}}{\partial x} = \mathbf{Q} \tag{13}$$

the quasilinear form of which is

$$\frac{\partial \mathbf{U}}{\partial t} + \mathbf{A}\frac{\partial \mathbf{U}}{\partial x} = \mathbf{Q}, \tag{14}$$

where $\mathbf{A}$ is the acoustic tensor. Operating on Eq. (14) with the inverse of the column eigenvector matrix gives

$$\frac{\partial \mathbf{W}}{\partial t} + \Lambda\frac{\partial \mathbf{W}}{\partial x} = \mathbf{E}^{-1}\mathbf{Q} \tag{15}$$

and, finally, we obtain the set of decoupled equations in the characteristic variables $\mathbf{W} = \mathbf{E}^{-1}\mathbf{U}$. In the computations, we evaluate the physical variables in the acoustic tensor using the arithmetic mean between nodes i and $i+1$. For the cases considered in the test problem, the arithmetic mean allows the flux term to accommodate arbitrarily large jumps, i.e., we have an approximate Riemann solver.

At this point we should mention that in most continuum mechanics codes, the energy equation is not included. This is the case for LAYER. The disadvantage of not having an energy equation is that estimates of heat (therefore entropy) are impossible. For complicated wave interaction problems, having the entropy can be very useful. For two-dimensional axisymmetric continuum mechanics problems, the hoop strain compatibility condition is superfluous. The radial strain does not affect the eigenvalues for the axial acoustic tensor, and, similarly, the axial strain does not affect those of the radial acoustic tensor. Lastly, the two nonzero off-diagonal terms in the strain tensor lead to only one nonzero eigenvalue. These terms are combinations of shear strain and rotation, and, in general, shear strain is the more important physical variable.

3. THE ENGQUIST FILTER

The version of the Engquist system filter used here is essentially the same as the algorithm reported in [12] for gasdynamics. The only difference is that more arrays are required for the four equations (Eq. 5) than for the three in gasdynamics. At each timestep, we filter the axial direction first and then the radial. In each direction, the filter first scans the particle velocity array to identify the extrema. Those nodes at or adjacent to an extremum will be filtered. If the extremum is a plateau, the nodes adjacent to the plateau will be included. Then the filter calls the characteristics routine to obtain the characteristic variables for those nodes. The filter re-scans the characteristic variables to determine if the physical extrema in the velocity field are reproduced in the characteristics fields, and, if necessary, corrections are made to each extremum in the characteristics arrays according to the criteria given in Algorithm 4.1 in [5]. The only modification we made is in the size of the correction δ (discussed in the next section). Afterward, the physical variables are calculated from the corrected characteristic variables. As mentioned in [5], because TVD is enforced in characteristics space, the physical variables may occasionally violate the TVD criterion. Indeed, in our numerical experiments, TVD is occasionally violated in the physical variables; however, the oscillations are small and usually do not persist for more than a few timesteps. Enforcing TVD for the physical variables is very costly. This is particularly true for solid mechanics and multi-dimensional problems. We have chosen to maintain a ''semi-TVD'' property in this filter.

4. MODIFICATION OF FILTER CORRECTIONS

We have previously noted that, in the two-dimensional case being treated in the present study, it has been necessary to alter the factor that multiplies the correction δ from its usual value of 0.5 to a lower value of 0.15. The latter value was determined via numerical experiments and was required to avoid a ''stair-stepping'' anomaly of the basic filter for a decaying wave. We emphasize that this modification is essential to the success of the filter for multi-dimensional problems because most of the waves in multi-dimensions are decaying waves. Because this ''stair-stepping'' anomaly and the modification we introduced have not been studied or mentioned by Engquist *et al.* [5], we will provide an heuristic discussion concerning this modification, and its relation to the flux modification of TVD.

In the original Engquist filter, corrections are often made to reduce the difference between v_j and v_{j+1} to zero, where j is

the location of the extremum. This is achieved by correcting the larger value by $-\delta|v_j - v_{j+1}|$ and the smaller value by $+\delta|v_j - v_{j+1}|$ and setting $\delta = 0.5$. For a step wave, where the stresses behind the wavefront are constant, the correction $\delta = 0.5$ is acceptable because this correction flattens the extrema. For a decaying wave, the stresses behind the wavefront decreases with distance away from the front. The correction of $\delta = 0.5$ will cause some of the filtered extrema to flatten, leading to the shape of a staircase behind the shock. An example is given in Section 6.

Engquist *et al.* [5] show that it is possible to express their postprocessing conservative filter formulation in terms of a flux modification procedure by writing the corresponding (filtered) numerical fluxes as

$$F_f = F_j + \frac{1}{\lambda}\zeta(r_{j-1})\,\Delta_- v_{j-1}^{(j-1)} + \frac{1}{\lambda}\zeta\left(\frac{1}{r_j}\right)\Delta_+ v_j^{(j)}, \qquad (15)$$

where, following [5], we have

$$r_j \equiv \frac{\Delta_+ v_j^{(j)}}{\Delta_- v_j^{(j)}}, \qquad \lambda = \Delta t/\Delta x \qquad (16)$$

and $\zeta(r)$ is defined as

$$\zeta(r) = \begin{cases} 1, & r < -2, \\ -r/2, & -2 < r < -1 \\ \frac{1}{4}, & r = 1 \\ 0, & r > -1. \end{cases} \qquad (17)$$

We note that subscripts j indicate grid point indexing and parenthesized superscripts (j) denote the filter iteration step. The symbols Δ_+ and Δ_- denote forward and backward differences.

It is clear from the forms of (15) and (17) that differencing of F_f will result in some dissipation whenever $r \le -1$ and that the actual amount of this dissipation depends on r only for $r \in (-2, -1)$; otherwise the dissipation is either zero or is simply proportional to $\Delta_- v_{j-1}^{(j-1)}$ and $\Delta_+ v_j^{(j)}$. In any case, in two dimensions we have found that the amount of dissipation arising from (17) is not always correct. Furthermore, in the case $r \in (-2, -1)$, the factor of $\frac{1}{2}$ multiplying $-r$ in the definition of ζ is precisely the value of the correction step multiplier ($\delta = 0.5$), as can be deduced from Algorithm 2.1 of [5]. In particular, then, reducing the value of this multiplier will result in a reduction of the level of artificial dissipation, as is easily seen from Eq. (15).

From this, it is evident that the action of this factor leads to behavior similar to that induced by the parameter θ in Harten's TVD schemes [1]. As noted in [1], such alteration of the numerical viscosity seems to be necessary in multi-dimensional problems whose solutions contain contact discontinuities (linearly degenerate characteristic fields). In addition, it is observed that this factor can be employed to improve resolution in general. It is not our intent in the present paper to provide a detailed analysis of the correspondence between θ and the correction step multiplier of the Engquist filter. Rather, we wish to simply point out the similarities to provide a justification for the modifications we have made to the filter during the current study, leaving the rigorous analysis of this for future work.

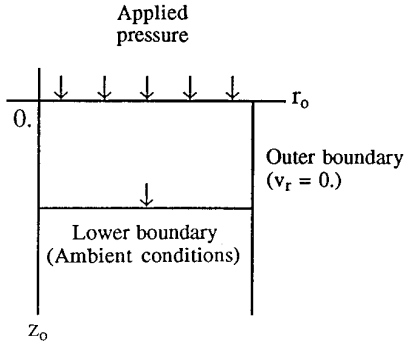

FIG. 2. Initial and boundary conditions for the planar shock problems.

5. THE TEST PROBLEMS

After the filter and the characteristics routines are implemented into LAYER, we applied the code to two test problems; the configuration is shown in Fig. 2. The first one is the propagation of a planar stress wave in a half space of a linear elastic solid. We limited the outer radius of the problem to a small value and applied a zero radial velocity boundary condition at the outer boundary. Because the problem is linear, the performance of the nonlinear filter for a linear wave propagation problem can be examined.

The second problem is the propagation of a planar shock in a bilinear solid. Figure 3 shows the stress–strain relations for a bilinear solid. There are two bulk moduli and therefore two wavespeeds, one for loading and the other one for unloading.

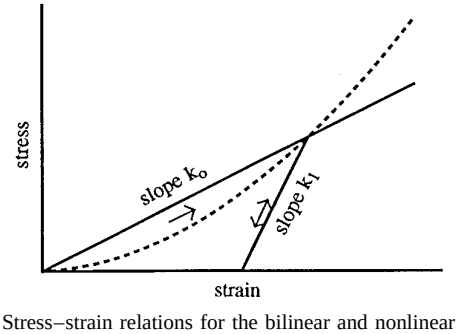

FIG. 3. Stress–strain relations for the bilinear and nonlinear materials.

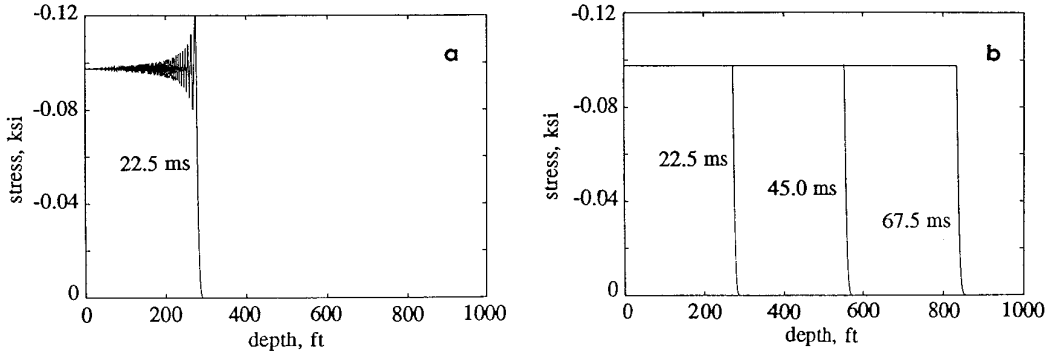

FIG. 4. Solutions to the planar step wave problem: (a) The unfiltered finite-difference solution for $dz = 1$ ft., and $q = 0$; (b) The filtered finite-difference solution for $dz = 1$ ft and $q = 0$.

The analytical solution to this problem, given by Salvadori *et al.* [13] simplifies to the following form. The stress is given by

$$-\sigma(x, t) = p\left(t - \frac{x}{c_1}\right) + G\left(t - \frac{x}{c_1}\right) - G\left(t + \frac{x}{c_1}\right) \quad (18)$$

and the velocity is given by

$$\rho c_1 v(x, t) = p\left(t - \frac{x}{c_1}\right) + G\left(t - \frac{x}{c_1}\right) + G\left(t + \frac{x}{c_1}\right), \quad (19)$$

where

$$G(t) = \sum_{m=1}^{\infty} \varphi^m p(\varphi^m t) \quad (20)$$

with $\varphi = (c_1 - c_0)/(c_1 + c_0)$, where c_0 and c_1 are the sound speeds corresponding to the loading and unloading moduli, respectively. For our test problem we chose

$$p(t) = \frac{p_0}{1 + t/t_0}, \quad (21)$$

where t is the time and t_0 is a decay constant. For the calculations, we used $p_0 = 0.1$ ksi and $t_0 = 0.1$ s.

6. RESULTS

The filter works extremely well for the linear problem. Figure 4 shows the wave profile for this step wave with and without the filter. In the numerical experiments, we found that there is an optimum choice of grid spacing such that the amount of dissipation in the underlying grid is just the right amount for the filter to operate efficiently. For extremely small grid sizes, less than a centimeter for this problem, the numerical oscillations will grow even when we filter the solution. On the other hand, if the dissipation in the underlying grid is too high, the filter has a tendency to turn the front from a gradual rise into a step and eventually causes the calculation to go out of bounds in doing so. We have performed a convergence study for this case and obtained a convergence rate of 0.7 in the L^1-norm.

Figure 5 shows the results for Problem 2. The case of zero artificial viscosity ($q = 0$) without the filter (Fig. 5a) shows large oscillations. In this case, the filter is able to suppress the oscillations as soon as they appear, before they grow to any significant magnitude (Fig. 5b). Figure 5c shows the analytical solution. The filtered solution requires 50% more computing time than the no-filter case. The numerical convergence test shows a convergence rate of 0.6 in the L^1-norm for this planar shock case. For this problem, $\delta = 0.15$ is used. If $\delta = 0.5$ is used, stair stepping will appear behind the shock (Fig. 6). For the linear step wave problem, our numerical experiments show that the solution is unchanged for values of δ between 0.1 and 0.5, which suggests that the value for δ does not have to be as high as 0.5. The optimal value, in the interest of minimizing the amount of artificial dissipation, is closer to 0.1.

We performed the above-mentioned grid function convergence tests for two reasons. The first is that a convergence proof for the case of systems of equations is not available. It is good practice to verify that reasonable convergence rates are achieved whenever the system of equations is changed. In this case, we changed from the gasdynamics equations to the small-strain equations for solids. The second reason is that because we modified the Engquist filter (Section 4), it is important to demonstrate that convergence is achieved in the modified filter. Because the resulting convergence rates are similar to those we obtained for 2D gasdynamics calculations, we conclude that very little penalty is associated with changing to the small-strain equations and introducing the modification.

Encouraged by the results of the two test problems, we proceed to solve the problem of a decaying planar shock propagating in a nonlinear material. This material has a quadratic stress–strain relation for loading (concave upward in Fig. 3) and a linear unloading modulus. Figure 7 shows the calculated shock at the same times as in the bilinear case. Note that the shock in the nonlinear material travels a bit slower than that in the

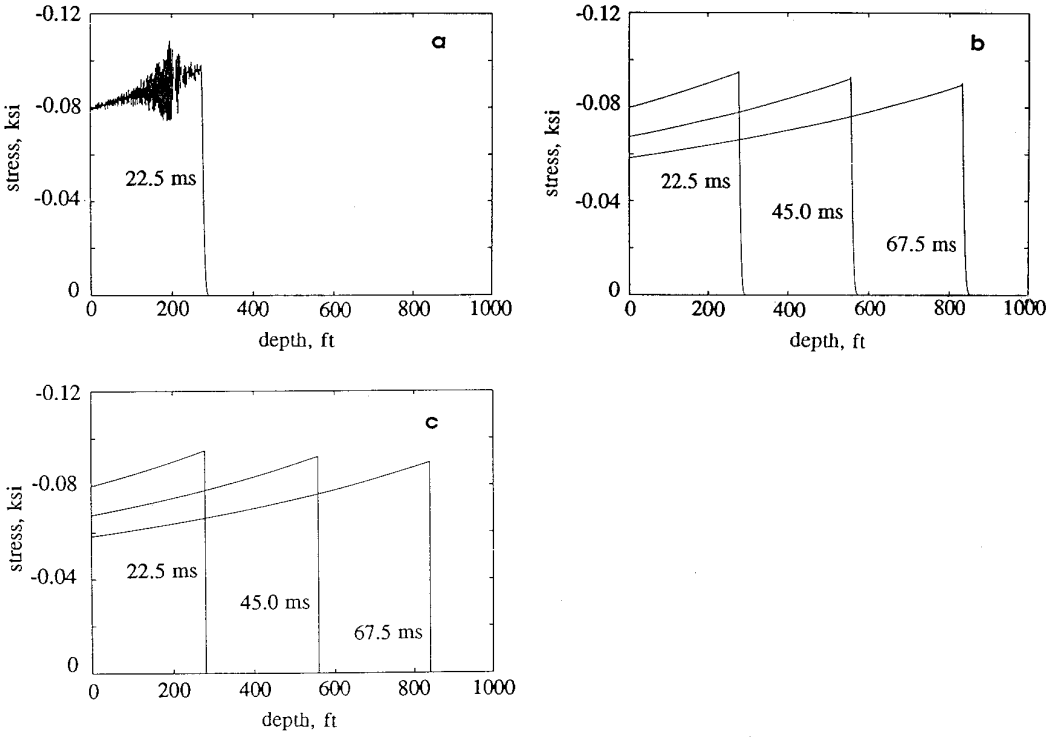

FIG. 5. Solutions to the bilinear problem: (a) The finite-difference solution for $dz = 1$ ft and $q = 0$; (b) The filtered finite-difference solution for $dz = 1$ ft and $q = 0$; (c) The analytical solution.

bilinear material due to the quadratic stress–strain relation. Figure 8 shows the grid function convergence of the filtered solution for both the bilinear and the nonlinear cases. For the bilinear case, Fig. 8a, the filter is able to eliminate the Gibbs oscillations even for the smallest grid spacing. However, the number of grid points needed to effect the transition at the shock front increases as the grid spacing is reduced. For this, as well as the linear elastic problem, the sharpness of the front is determined by the initial development of the front at the free surface, where the loading is applied. The constant loading modulus ensures the same propagation speed for the initially calculated front; therefore, the number of grid points needed to effect this transition cannot be reduced. By eliminating the Gibbs oscillations, however, numerical convergence can be achieved. The calculated front does steepen in physical dimensions as the grid spacing is reduced, as shown in the figure.

For the quadratic case, Fig. 8b, the shock front is typically resolved in 5 to 6 grid points. This is clearly not as good as a 1D problem for which our experience suggests only 2 to 3 grid points are necessary to resolve the shock. However, considering that this is a 2D calculation, resolving the shock in 5 to 6 grids is quite remarkable. In general, the radial stresses and velocities are five to six orders of magnitude smaller than those of the axial.

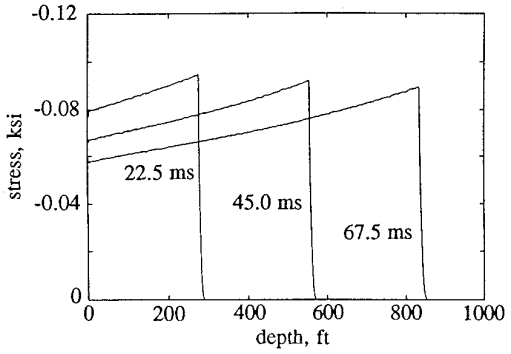

FIG. 6. Typical ''stair-stepping'' in the filtered solution using $\delta = 0.5$.

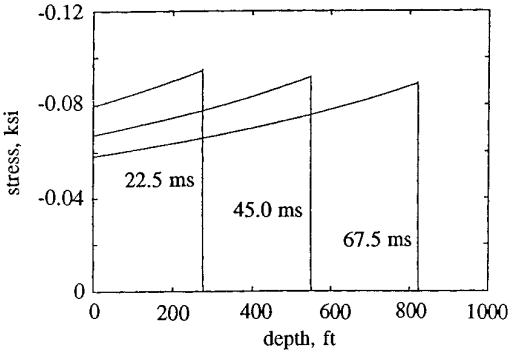

FIG. 7. Solution to the nonlinear problem $dz = 0.25$ ft and $q = 0$.

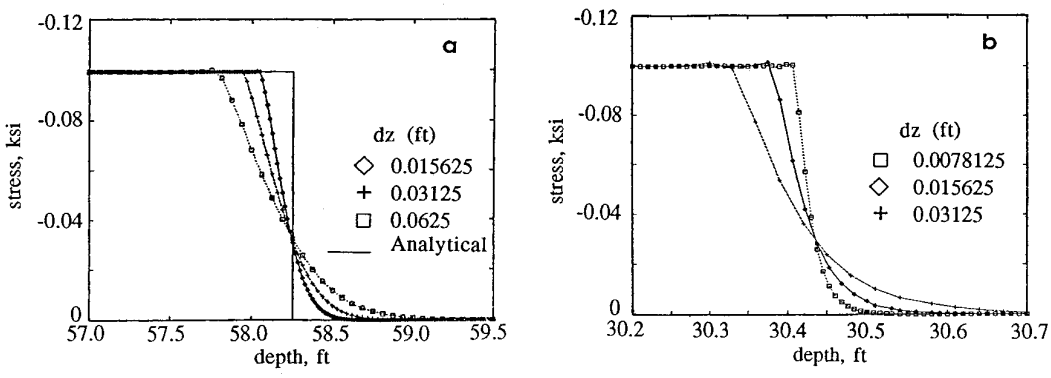

FIG. 8. Grid solution: (a) The bilinear problem; (b) The nonlinear problem.

7. CONCLUSION

We conclude that the Engquist filter can be used to improve the finite-difference solutions to a class of continuum mechanics problems involving wave propagation in linear elastic, bilinear elastic, and nonlinear solids. However, the original Engquist filter must be modified when applied to decaying waves. This modification is essential to the success of the filter when it is applied to multi-dimensional problems in both gasdynamics and solid mechanics. In particular, the modification reduces the amount of artificial viscosity added to the solution at locations chosen by the filter. The filtered plane wave and decaying shock have sharp fronts and very little oscillation behind the fronts. Grid function convergence tests indicate convergence rates of approximately 0.6 in the L^1 norm for all the cases considered in this study. As expected, the convergence rate is reduced to approximately first order at the shock even though the scheme is second order away from discontinuities.

ACKNOWLEDGMENTS

This work was supported by the Defense Nuclear Agency under Contract No. DNA-001-93-C-0138. We thank Dr. Randy Rohr of the Defense Nuclear Agency for his support and encouragement, Dr. Ivan Sandler (Weidlinger Associates) for his guidance on the LAYER code, and Dr. Don Simons (Logicon RDA) for providing the simplified analytical solution to the bilinear problem.

REFERENCES

1. A. Harten, *J. Comput. Phys.* **49,** 357 (1983).
2. S. T. Zalesak, *J. Comput. Phys.* **31,** 335 (1979).
3. P. Colella and P. R. Woodward, *J. Comput. Phys.* **54,** 174 (1984).
4. A. Harten and S. Osher, *SIAM J. Numer. Anal.* **24**(2), 279 (1987).
5. B. Engquist, P. Lodstedt, and B. Sjogreen, *Math. Comput.* **52,** 509 (1989).
6. F. Lafon and S. Osher, *J. Comput. Phys.* **96,** 110 (1991).
7. R. F. Warming, R. M. Beam, and B. J. Hyett, *Math. Comput.* **29,** 1037 (1975).
8. P. L. Roe, *J. Comput. Phys.* **43,** 357 (1981).
9. S. S. Antman and W. G. Szymczak, *Contemp. Math.* **100,** 27 (1989).
10. J. A. Trangenstein and P. Colella, *Commun. Pure Appl. Math.* **44,** 41 (1991).
11. D. Rubin and I. S. Sandler, U.S. Army Corps of Engrs. Rept. SL-89-1, 1989 (unpublished).
12. C. K. B. Lee and J. M. McDonough, *J. Comput. Phys.* **117,** 289 (1995).
13. M. G. Salvadori, R. Skalak, and P. Weidlinger, *J. Eng. Mech. Div. Proc. ASCE* **77** (1960).